Review

A review of the design and performance characteristics of a horizontal wind turbine using numerical methods

Firstname Lastname [1], Firstname Lastname [2] and Firstname Lastname [2,*]

[1] Affiliation 1; e-mail@e-mail.com
[2] Affiliation 2; e-mail@e-mail.com
* Correspondence: e-mail@e-mail.com; Tel.: (optional; include country code; if there are multiple corresponding authors, add author initials) +xx-xxxx-xxx-xxxx (F.L.)

Received: date; Accepted: date; Published: date

Abstract: Renewable energy technologies are receiving much attention to replacing power plants operated by fossil and nuclear fuels. Amongst the renewable technologies, wind power was successfully implemented in several countries. There a number of parameters in the aerodynamic characteristics and design of the horizontal wind turbine. This paper highlights the key sensitive parameters that affect the aerodynamic performance of the horizontal wind turbine, such as environmental conditions, blade shape, airfoil configuration and tip speed ratio. Furthermore, this paper introduces the recent control system used for the horizontal wind turbine. Different turbulence models applied to predict the flow around the horizontal wind turbine using Computational Fluid Dynamics modeling are reviewed. Finally, the challenges and conclusion remarks for research directions in the design of the wind turbine are elaborated.

Keywords: Horizontal-axis wind turbine (HAWT), airfoil, Performance, Turbulence model, Computational Fluid Dynamic (CFD).

1. Introduction

Energy demands are increasing with the world's population and industrial growth [1]. Consumption of energy is predicted to increase by 56% from 524 BTUs in 2010 to 820 BTUs in 2040 [2]. The extensive consumption of fossil fuels is the primary source of carbon dioxide emission to the atmosphere. The CO_2 released from fossil fuel burning is estimated to increase from 1,000 million metric tons in 2010 to 36,000 million metric tons in 2020, and may reach 45 billion metric tons by the end of 2040 [3].

The demands on clean energy sources have been increased rapidly due to environmental awareness, decreasing reliance on traditional fuel origins, and strict environmental policies [4]. Amongst all renewable energy sources, wind energy seems to be one of the popular raising technology due to its low prices and its rapid global development [5]. The total world installed power from wind energy increased from 296,581 MW in 2013 to 597,000 MW at the end of 2018, and it is predicted to reach 817,000 MW by 2021 [3].

The World Wind Energy Association updated that the statistic of the added wind capacity during 2018 was around 50.1 GW, which is slightly less than the installed wind energy capacity in 2017, as shown in Figure 1(a). The installed wind capacity in 2017 achieved the third largest installation level during one year after record numbers in 2015 and 2014. On the other hand, 2018 exhibited the lowest market growth rate, about 9.1%, since the growth of wind turbine technology at the beginning of the twentieth century, as shown in Figure 1(b). In 2018, the most significant contributing countries to wind turbine energy were China (34.81%), USA (16.48%), and Germany (10.41%), as shown in Figure 2 [3].

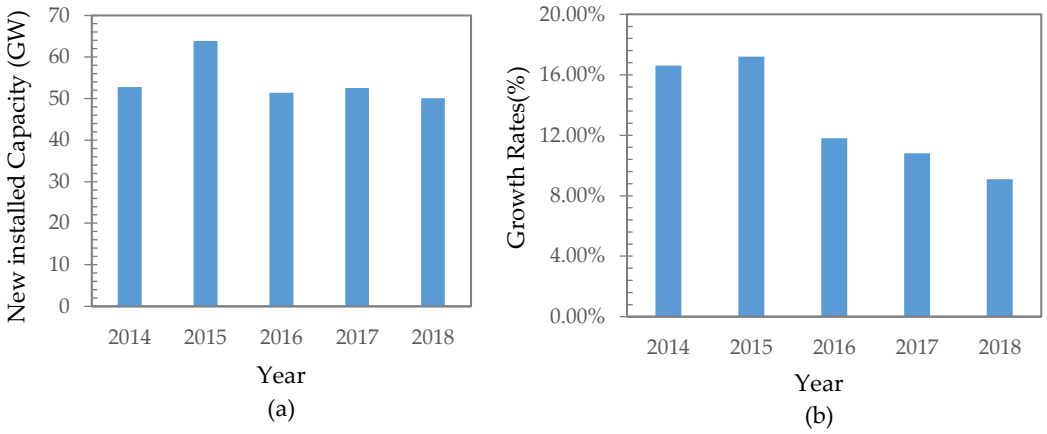

Figure 1. (a) New installed capacity of wind energy and (b) growth rate of wind energy.

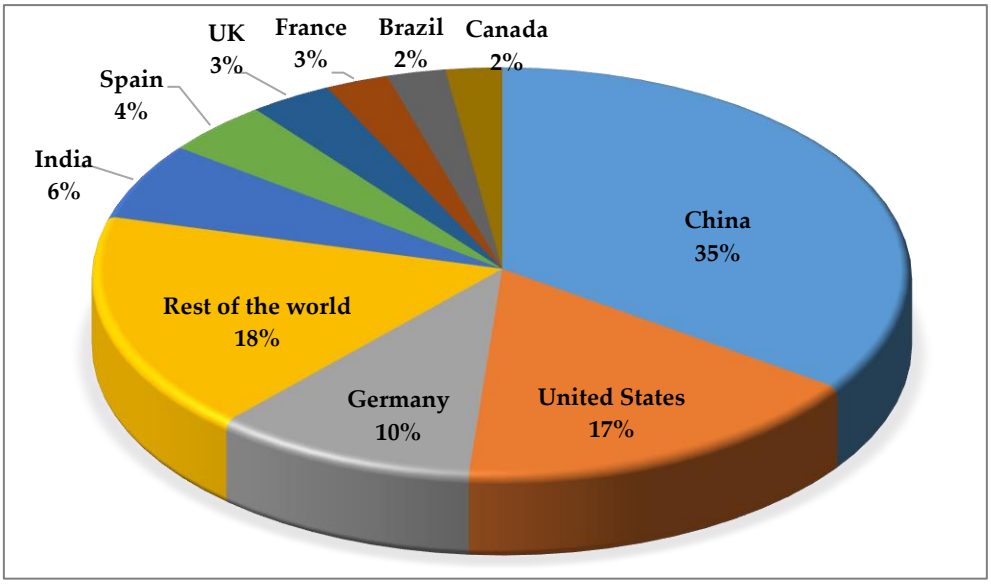

Figure 2. The sharing percentage of the countries in the worldwide wind energy market at the end of 2018.

[6] reviewed the modelling of wind turbine power curves using the different methodologies employed for control the wind turbine power curve. [7] presented a general review and classification of wind turbine condition monitoring technics and methods with a concentrate on trends and future challenges. [8] discussed a study wake effects on downstream turbines using different fluid dynamics techniques. This paper aims to highlight sensitive parameters, which affected the aerodynamic design aspects and performance characteristic of the horizontal wind turbine. The optimization of operating parameters of wind turbine design has significant impacts on the amount of energy output. Regarding the optimization of the power output, recent different control methods used discussed. Furthermore, this paper examines the Computational Fluid Dynamics techniques (CFD) are used for solving flow problems around wind turbines, where a review of turbulence models used for aerodynamic simulation of the wind turbine studies are presented.

The paper reviewed sensitive parameters affecting the design and performance of the horizontal wind turbine and examined the associated aerodynamic characteristics of different control systems

of the horizontal wind turbine. It also highlighted the various turbulence models and their applications in Computation Fluid Dynamic modelling to analysis of the aerodynamic characteristic of the horizontal wind turbine.

2. Sensitive parameters of design and performance of the horizontal wind turbine

There are several parameters, which influence the aerodynamic characteristic of HAWT, such as atmospheric conditions and the shape of the wind blade. Scaling up the capacity of the wind turbine requires an increase in blade length to maximize the energy output. Therefore, understanding the critical operating parameters on the performance of the wind turbine should be considered in the design of the expected power output. This section discusses the key design and operating parameters in the wind turbine.

2.1. Atmospheric condition (wind data models)

Wind speed plays a vital role in the performance of the wind turbine since it is the primary source of energy. The wind speeds at a specific site are varying with annual, seasonal, and daily changes. It is crucial, therefore, to describe these variations by different mathematical distribution models [9]. The high accuracy analysis of wind data is essential to encourage stakeholders, increasing the investment in wind energy technology. Statistical analysis methods such as probability distribution function were proposed for studied the potential of wind resources in a specific location. The probability density distribution describes the occurrence frequency of wind speed using common functions such as Rayleigh and Weibull [10]. Rayleigh probability distribution function requires only the mean wind speed; thus it is a simplistic probability distribution function $f(v)$ as described by equation 1

$$f(v) = \frac{\pi}{2}\left(\frac{v}{\bar{v}^2}\right) exp\left[-\frac{\pi}{4}\left(\frac{v}{\bar{v}}\right)^2\right] \quad (1)$$

where v is the wind speed (m/s) and is the average wind speed (m/s).The Weibull distribution function is considered as one of the common probability functions used in wind speed probability analysis. The Weibull probability function, as shown in equation 2, is depending on two factors, scale and shape factor [11, 12].

$$f(v) = \left(\frac{k}{c}\right)\left(\frac{v}{c}\right)^{k-1} e^{-\left(\frac{v}{c}\right)^k} \quad (2)$$

where k is the shape factor (dimensionless), and c is the scale factor (m/s). The curvature of the probability distribution function is decided by the shape parameter; any variation in the shape parameter is affected by the estimated wind potential. The Rayleigh distribution is used when the mean wind speed is only available for the location. Rayleigh distribution is a special case of Weibull distribution when the shape factor is equal to 2, and the scale parameter depends on the mean wind speed. More spread of wind speed probability functions is related to a lower shape factor[13].

Determination of the Weibull function requires defining the shape and scale parameters, using different estimation methods. Using the maximum likelihood method which is one of the familiar formula used for defining shape and scale parameters as seen in the following equations [14, 15]:

$$k = \left(\frac{\sum_{i=1}^{n} {v_i}^k \ln(v_i)}{\sum_{i=1}^{n} {v_i}^k} - \frac{\sum_{i=1}^{n} \ln(v_i)}{n}\right)^{-1} \quad (3)$$

$$c = \left(\frac{1}{n}\sum_{i=1}^{n} v_i^{\,k}\right)^{\frac{1}{k}} \quad (4)$$

where v_i is the wind speed at(i)time and n is the number of reading of wind speed data. In order to define the annual energy production of wind turbine *(AEP),* probability density distribution *f(v)* is combined with the power curve of wind turbine *P(v)* as shown in the following equation

$$AEP = \int_{v_{cut-in}}^{v_{cut-out}} P(v)\, f(v) dv \quad (5)$$

where v_{cut-in} is the cut-in wind speed (m/s) , and $v_{cut-out}$ is the cut-out wind speed (m/s).

In the energy market, the values of wind speed at different hub heights of the wind turbine are very desirable, according to unavailability recorded data from wind station measurements. To calculate the wind speed *v(h)* at different altitude values *(h)* which depend on the measured wind speeds at reference value using power exponent law as seen in the following equation [16] :

$$v(h) = v_o\left(\frac{h}{h_{ref}}\right)^{\alpha} \quad (6)$$

where v_o is the wind speed at reference height (h_{ref}) , and α is a power-Law exponent (dimensionless) which varies with time of the day, terrain nature, temperatures, and the season of the year [17]. The power-law exponent varies from 0.1 in smooth terrains to 0.40 in very rough terrains where a value of 1/7 could be used when no information about specific site formation.

Different studies have been analysed wind data using Weibull and Rayleigh probability distributions functions. For example, Islam et al. [18] assessed the potential of wind energy at Kudat and Labuan, Malaysia using Weibull distribution; the results showed unsuitable of these sites for commercial wind energy generation. Krenn et al. [19] studied the wind data in Austria for ten years, depending on station data combined with a hybrid geo-statistical model. The result indicated the feasibility of Weibull distribution in capturing the average annual wind speed with 0.8 m/s standard deviation of error. Celik [20] evaluated the potential of wind energy at the Mediterranean coast of Turkey based on Rayleigh and Weibull models. The results showed that the Weibull model gives better accuracy of the power density distribution compared to the Rayleigh model. In contrast, the Weibull model gives an annual average error of around 4.9% compared with 36.5% for the Rayleigh model when compared to wind speed measured reading. Mentis et al. [21] used the daily wind speed at different sites in Africa for one year by Weibull and Rayleigh distributions. The results showed 5% differences along with the results between Rayleigh and Weibull distribution, but the variation exceeded 100% at specific locations. As such, the Rayleigh model is not valid at those sites, especially on the country level, and it can be used for estimation wind energy probability on a continental level only.

2.2. The Shape of the wind turbine blade

The number of blades in wind turbines varies depending on the design [22-24]. Currently, the 3-bladed upwind horizontal wind turbine is the most popular modern wind turbine design due to its system efficiency, stability, and the feasibility of the economic issues of the wind turbine system. A horizontal wind turbine consists of majors components. The foundation component of the wind

turbine is the tower, which holds the nacelle. The nacelle contains the transmission system, generator, control systems. The transmission system transmits the mechanical torque from rotor to generator, which includes the gearbox, mechanical brake system [25]. The generator used electromagnetic components to convert mechanical power into electrical power [26-29]. The rotor component captures the wind power and converting it into mechanical torque. The rotor contains the blade component attached to the nacelle by the hub. Different materials are used in the manufacturing of wind turbine blades such as carbon-hybrid and S-glass [30, 31]. Various studies demonstrated that decreasing the rotor and nacelle weight will reduce the manufacturing costs. Still, this decrease has a dynamic aero-structural limitation and balancing issues that should be considered in the design [32, 33].

One of the most critical design parameters of the wind turbine is the determination of the airfoil chord length distribution along the wind turbine blade. There are different methods for determining the chord length, where the Betz optimization theory is considered as the most straightforward method, which gives reasonable approximation values of the chord length of the airfoil section [34]. This method approximates a good optimum value of blade chord length, which has a 6-8 tip speed ratio with neglecting losses from the tip and drag. Consequently, this method is inaccurate in some cases with low tip speeds, blade sections near the hub, and high drag airfoil sections [35-37]. The blade of the wind turbine is divided into three essential parts; root, mid-span, and tip based on the structural and aerodynamic roles. The larger chord length should be in the root area due to structural loads, while the slender airfoil sections will be in the tip region area. Thus, the area near the hub is responsible for the required starting torque, while most of the production torque is initiated from the tip region [38-42]. There is research area focuses on aerodynamic optimization of the shape of the wind turbine design. For example, Liu and Tang [43]studied the novel of optimization of fixed speed wind turbines using linearization of twist angle and chord profiles method. The result concluded that there is a good increment of the annual energy production when designing an optimal blade using linearization novel for wind speed range from 4-7 m/s.

2.3. Wind power curve and tip speed ratio

The power curve gives the power output of the wind turbine at each wind speed. This curve is essential for forecasting the performance of wind speed, which improves grid planning and connecting wind energy into the power systems [44]. The least wind speed required to deliver a useful power is called the cut-in speed while the turbine is shut down at the cut-out wind speed due to engineering safety to prevent damage from massive wind loads [45, 46]. Some of the methods used to enhance the aerodynamic performance of the HAWT over different wind speeds is by decreasing the cut-in wind speed. For example, Singh at el. [47]designed a wind turbine with a better start-up performance at low wind speed using a numerical method, which used to decrease the cut-in wind speed in addition to achieving a better combination of lift to drag ratios, which validated against experimental data.

The tip speed ratio is a key design factor, which affects the calculation of different design parameter of the optimum rotor dimensions. The definition of tip speed ratio is a ratio between the velocity of the rotor blade and relative wind speed. The aerodynamic design of the wind turbine is

sensitive to any changes in the tip speed ratio. Thus, a rotor blade design, which operated at relatively high wind speed, will generate a lower torque at minimum wind speed. Also, this rotor operating at high wind speed will increase the cut-in speed and self-starting difficulties [24]. Derakhshan et al. [48] tested the effectiveness of the shape optimization in their numerical study of the wind turbine. The study found that the optimization of chords distribution has increased by a percentage of 3.7 of the power of wind turbines at rated speed (10m/s). In contrast, the percentage of average power increased by 1.2%.

Selecting an appropriate tip speed ratio should take into account the design of different parameters such as output torque, mechanical stress and efficiency, aerodynamic characteristic, and noise [49]. Practically, raising the tip speed ratio will increase the noise to the sixth power [50]. In order to yield an efficient mechanical to electrical conversion, the tip speed ratio should be six to nine for modern three-blade wind turbine and nine to ten for two-blade wind turbine [51].

2.4. Airfoil configuration

2.4.1. Conventional airfoil

An efficient blade design is formed from different airfoil profiles with a blending at an angle of twist for each airfoil terminating at a circular blade root. Different simplification is used to smooth and facilitate industrial production and cutting-down the manufacturing cost, such as minimizing the numbers of varying airfoil profiles, linearization of chord width, and decreasing the twist angle [52]. The decision to select airfoils has a critical role in the output torque from a wind turbine. The direct impact of airfoil design defines the aerodynamic performance of wind turbines. The lift to drag ratio is an essential aspect of the aerodynamic characteristics of the airfoil. Over the past decade, there were several experimental works for testing lift and drag coefficients of airfoils with different Reynolds numbers and angles of attack [53, 54]. The angle of attack is a very sensitive parameter for calculating the drag and lift coefficient of the airfoil. This angle is evaluated as the difference between the flow angle and the rotor plane angle. Therefore, the most important factor in the design of the wind turbine is to maximize the lift to drag ratio [54, 55].

The power output in a horizontal wind turbine is affected mainly by the lift to drag ratio of the airfoil, which is usually designed to operate at a low angle of attack where the lift coefficient is often much higher than the drag coefficient [53]. Different airfoil families have been used in the design of modern wind turbines such as NACA sub-families four and five-digit, for example, NACA 65-415, NACA 63-215 [56]. NACA is developed by the National Advisory Committee for Aeronautics predecessor of NASA, USA. The NACA airfoils are usually appropriate for situations where the angle of attack is relatively small, and Reynolds number is high [57]. NACA 63 and 44 series are known for their characteristics of stall delay and lower sensitivity to roughness in leading-edge than other families [58]. Yılmaz et al. [59] investigated the aerodynamic efficiency of the wind turbine blade by experiment, and results were compared with a numerical simulation. The study selected NACA 4420 airfoil for analysis and showed the dependency of the efficiency of HAWT on the blade profile.

RISØ-A-XX is another family used in the design of the wind turbine blade and has been developed and optimized by RISØ National Laboratory in Denmark [60-62]. Direct numerical optimization is used to describe the airfoil shape that optimizes with a B-spline representation. The family has contained seven airfoils that varied in relative thickness to chord from 12% to -30%. The

DU series airfoil family is another airfoil family, which was developed by the Delft University of Technology, Netherlands. The relative thickness to the chord of DU series airfoil varies from 15% to 40%, for example, DU 91-W2-250 and DU 93-W-210, which has an airfoil thickness of 25% and 21% respectively [63].

There are many airfoils used for wind turbine design; for example, the Aeronautical Research Institute of Sweden develops the FFA airfoil family [56]. Also, the S airfoil family is developed by the National Renewable Energy Laboratory (NREL) [64, 65]. Some considerations should be taken in determining the type of airfoil used in wind turbines such as achieving a maximum lift to drag ratio, dynamic and structural requirements, and the sensitivity of airfoil for the environmental condition. Using one airfoil profile along the whole wind turbine blade gives a lower efficiency for the blade design. In some applications, different airfoil shapes can be used in the design of a wind blade, but blending between these airfoils in the design process would increase the efficiency.

The sections of an airfoil with high thickness to chord length ratio are usually used in the root region according to structural load requirements [61]. However, airfoils of high thickness have a lower value of lift to drag ratio. Therefore, significant research efforts were made to increase the lift coefficient of the thick airfoil used in wind turbine design. In the tip regions, the aerodynamic characteristic is critical to maximizing the lift to drag ratio, which explains using thin airfoil in the tip region.

In large modern wind turbine blades, the inboard and mid-span regions are used airfoils that had a relative thickness of 25% or above, for example, FFA- W3-241 and FFA-W3-301 airfoils are used inboard and mid-span regions due to relatively high thickness [66]. S809 and S814 airfoils are recommended for the tip region of the wind turbine, which had a blade length that varies from 10 to 15 m [67]. Different studies are focusing on the investigation of different airfoils in wind turbine design; for example, Van Rooij et al. [68] used Risø, DU, NACA, FFA, and S8xx airfoil families to investigate the performance of those airfoils to meet the aerodynamic and structural requirements. For airfoils of relative thickness to chord of 25% and 30 %, the best performing airfoils are S814 (24%), DU 91-W2-250 (25%), Risø-A1-24 (24%) where the performance differences between those airfoils are relatively small. While for airfoil thickness of 30 %, the DU 97-W-300 meets the most excellent performance according to restricted requirements.

Recently, a lot of work concentrated on designing blades for wind turbine rotors depending on maximizing the aerodynamic performance [69-71]. The generated power of a wind turbine varies with the speed and turbulence of the wind. Many countries have low wind speed in some locations. There is a lot of research in the development of small wind turbines to meet the energy needs of such countries. Ahmed et al. [72] studied lift, drag coefficient, and flow behaviour of SG6043 at low Reynold number to assess the airfoil aerodynamic characteristics used in wind turbines for regions having wind speeds of 4-6 m/s. The results showed that increasing the freestream turbulence level from 1% until 10% will not significantly change the lift coefficient. However, with an increasing angle of attack, the separation was delayed from the upper surface, which reflects on increasing the lift coefficient and reduce the drag coefficient. When the angle of attack increases, the lift to drag ratio also increases from 8% to 15% because of rising the turbulence level. Sayed et al. [73] simulated the aerodynamic performance of different S-series in low wind velocities. The study found that S825, S826, S830, and S831 airfoils are the most efficient in S-series for low and high wind velocities because they give a maximum lift to drag ratio, which achieves maximum power.

Airfoil characteristics such as flow separation vary with the level of wind turbulence [74-76]. Thus, many models combine the lift coefficient of the airfoil with delay flow separation [77]. Hoffmann [78] investigated the impact of changing the wind turbulence intensity of NACA 0015 from 0.25% to 9% at Re=250,000. The study found that the effect of delayed flow separation on increasing the maximum lift coefficient increase the angle of attack. It also found that the impact on delayed flow separation and increasing the peak lift coefficient due to changing turbulent intensity. Kamada et al.[79] discussed the dynamic and static characteristics at Re=350,000 for DU93-W-210 at two different turbulent intensity levels. This airfoil had 21% relative thickness, which tested in a wind tunnel with a turbulence grid that used to obtain a high turbulent flow. They observed a delay in flow separation when increasing the level of freestream intensity, which reflected on increasing the stall angle of attack.

2.4.2. Flatback airfoil

There are several attempts to improve annual energy production (AEP) by increasing the blade length [80]. Manufacturers have also researched to decrease the aerodynamic and structural load, which causes a long blade [81]. Researchers have proposed flatback airfoils at the inboard section of the blade due to the high lift coefficient and larger sectional area to overcome the disadvantages of the structural load caused by increased blade length [82, 83]. Kim et al. [84] studied the sufficient structural stiffness and safety consideration effect for flatback airfoil that have 20% cross-section areas larger than non-flatback airfoil. In addition, the rigidity of the cross-section area has increased due to a decrease in blade weight [85, 86]

The wealth of research in wind turbine applications using a flatback airfoil includes aerodynamic characteristics, design process, and simulation methods [87-91]. Murcia and Pinilla [92] investigated the adding thickness and cutting method in the design of flatback airfoil. Both methods showed an increase in maximum lift coefficient and drag coefficient, where the stall angle is delayed. However, adding thickness method gives a higher maximum lift coefficient when compared with cutting techniques. Standish and Van Dam [93] investigated the design process used in the flatback airfoil. The study concluded that the method of adding asymmetrical thickness on the baseline of the airfoil has an improvement on the changes of the aerodynamic characteristic of the flatback airfoil that produces after using cutting methods. As such, combined adding asymmetrical thickness design process decreases the negative effect of increasing thickness, which contributed to the cutting method, which will improve the aerodynamic characteristics of the airfoil.

Law and Gregorek [94] studied a flatback airfoil for a large capacity wind turbine. They found that a higher lift coefficient and the lower drag coefficient is achievable in a flatback airfoil compared to the conventional airfoil. Homsrivaranon found that using flatback airfoils enhanced aerodynamic performance by increasing the lift-to-drag ratio. Chen et al.[95]used a genetic algorithm for two desired optimization objectives (maximum lift coefficient and maximum lift to drag coefficient) to produce optimal flatback airfoil that have excellent aerodynamic properties. Zhang et al. [96] compared the different the numerical parameterization methods used for optimizing the airfoil; the results showed an improvement of lift-to-drag ratio. Still, there was no improvement for stall characteristics. Baker et al. [97]verified experimentally that insensitive of trailing edge flatback airfoil to contaminations on the leading edge, but the base drag in the wake caused drag increasing. Furthermore, the method of adding asymmetrical thickness on the baseline of airfoil improved the lift coefficient when compared with conventional airfoil, but the drag coefficient is increased.

Some of the drawbacks of the flatback airfoil compared with conventional airfoil are increasing drag at a high angle of attacks due to separation vortex [98]. A flatback blade generates separation vortex around the hub in the spanwise direction, so some of the essential research areas in the development of wind turbine blade are adding devices that suppress separation vortex, for example, vortex generator [99-101]. Ceyhan et al. [102] investigated the problem of the higher drag coefficient of flatback airfoils, which limits their structural application in inboard parts of the blade of the wind turbine. They suggested the swallowtail concept as a non-conventional flatback airfoil. They studied the modified DU 97-300 flatback airfoil experimentally with 10% trailing edge thickness and without the sallow tail. They found that the drag decreased 40%, and hence the output power of the wind blade could increase without any modification of operating conditions. Therefore, non-conventional flatback is a promising technology that could be used in the inboard part of the wind turbine. The other drawback of the flatback airfoil is increasing vortex shedding noise and aero-elastic problems [103, 104]. However, the inboard region in the blade, which used flatback airfoil, operates at speed lower than tip speed, this makes a slight increase of rotor noise.

3. Control system and associated performance characteristic

Wind energy is an uncontrollable resource of energy since wind flows randomly with time. The unsteadiness of wind flows explained the need for a control system that captured wind power with an efficient energy conversion system [11]. The main goals of using a control system in HAWT are increasing power production and decreasing static and dynamic structural loads by regulating the operating parameters to the desired value. Available wind power can be calculated according to equation 7 [105].

$$P_W = 0.5\rho A_r v^3 \quad (7)$$

where ρ is the air density and A_r is the rotor swept area. The power coefficient concept used as a significant factor in aerodynamic characteristic as the efficiency of the blade, which calculated as follows:

$$\mathrm{Cp} = \frac{P_m}{P_w} \quad (8)$$

where P_m is the mechanical power, C_n is a power coefficient (dimensionless). The angle of attack in the horizontal wind turbine will be increased by increasing the wind speed. Thus the dynamic stall phenomenon results according to unsteadiness variation of the angle of attack through the blade [106]. There are two different types of control systems are used for regulation the power in order to avoid stall conditions, stall regulated, and pitch regulated. The essential role of pitch regulated control system is a power regulation in the operating zone when the wind speed is higher than the rated wind. This regulation decreased the severe load on structural HAWT [107]. Recently HAWT is used as an active pitch control system with hydraulic and electrical actuators to overcome power fluctuating drawbacks [108].

The main controlled performance parameters in the HAWT are pitch angle and the generator torque. The rotor speed will vary accordingly to undergo the strategy of the

maximum power point tracking in the generator torque control system. On the other hand, in the pitch-regulated system, the smooth output power will result from the controlling of wind input torque. Controlling the optimum blade pitch angle and optimum tip speed ratio are used to get the optimum power coefficient in pitch regulated variable speed horizontal wind speed as there is an optimum power coefficient related to specific wind speed [109].

There are different control methods used. For example, the Maximum Power Point Tracking (MPPT) method is easily implemented as a control system; however, this method results in significant fluctuations in the load that is reflected in decreasing the wind turbine components life [110]. There is another technology used for the control system of rotor speed called LIDAR (Light Detection and Ranging) [111], which measured the wind speed ahead of the rotor blade then control the wind speed when the change of wind speed gradually. However, this method is not accurate under turbulent wind weather. Different research work on optimal control strategy used for increasing the efficiency of power production in [112, 113].

4. Computational Fluid Dynamic techniques

In the early 1990s, Computational Fluid Dynamics techniques (CFD) are used for solving flow problems around wind turbines by available commercial software, for example, EllipSys3D and Fluent [114-116]. The environmental conditions, e.g. wind speed and direction, have an essential influence on the lifetime of the wind turbine. Understanding the turbulence model, which simulates the aerodynamics of wind flow around a wind turbine, is essential for obtaining reliable results. In this section, different turbulence models for all flow Navier-Stokes equations are will be discussed. In CFD techniques, the method of finite volume is used for solving the momentum and mass equations in addition to equations of turbulence for each control volume cells.

4.1. Turbulences models

Until now, there is not a unique model that predicts all physical characteristics of turbulent flow. There are various models used in the turbulent flow of wind turbines such as Direct Numerical Simulation (DNS), Reynolds Averaged Navier-Stroke (RANS), and Large Eddy Simulation (LES). DNS has the highest accuracy in turbulence solution. However, the required computational time and cost are relatively high [117, 118]. The most common model used for solving Navier-Stokes equations is RANS [119, 120]. The mathematical principle concept is based on the calculation method of the Navier–Stokes equation, which divides the flow into a fluctuating part and average part where the average equation is called Reynolds-averaged Navier- Stokes equations. There are different turbulence models used for solving the RANS equation.

Firstly, the k-ε turbulence model series calculate the eddy viscosity by solving two parameters, the turbulent dissipation rate (ε) parameter, and a turbulence kinetic energy (k) parameter. Standard k-ε was specified by Launder and Sharma [121], which is widely popular used, but it gives poor results for flow that had a separation phenomenon such as flow around the wind turbine. Another improvement and modification on standard k-ε have been done to get the Renormalization Group *(RNG) K-ε* and *Realizable k-ε* turbulence models [122, 123]. Both models share the same

transport equation as standard k-ε for turbulent kinetic energy *(k)* and dissipation rate *(ε)*. However, the turbulent viscosity generation and calculation method are the differences among these models. The renormalization group theory was used as a statistical way for solving the *RNG k –ε* turbulence model. The *RNG k-ε* turbulence has different modifications than standard *k-ε*, for example, considering the impact of rotation in eddy viscosity. The *RNG k –ε* is more accurate, and has a better prediction for separations flows of the recirculation length than standard *k-ε* [124]. The realizable *k-ε* model is recommended for rotating bodies as the results could be improved when compared with standard *k-ε* for swirling flow problems under specific Reynolds numbers [125].

k-ω turbulence model is another RANS that is widely used for simulation flow around the wind turbine. Kolmogorov proposed the first form of the *k-ω* model [126]. The Imperial College group has done a new improvement in this model, but the most distinguish development has been done by Wilcox [127]. In some applications, the *k-ω* model has higher accuracy than *standard k-ε due to* boundary layers with an adverse pressure gradient, and the sublayer could be integrated without a need for any extra damping functions. However, *k-ω* is still sensitive for some flow with free stream boundaries applicant. *k-ω* Shear Stress Transport (*SST*) is an advanced turbulent model done by Menter [128], wherein this model combines the advantages of *k-ω* and *k-ε* turbulence model. Therefore, the inner part of the boundary layer where is used the *k-ω* models and then converted gradually to *k-ε* in the free shear layer and wake region outer layers. The translation between the two models is related to blending functions. The other advantages of this model are the modification of eddy viscosity, which considers the effect of turbulent shear stress transportation. Different modifications of *k-ω* Shear Stress Transport (*SST*) had been done to enhance rotation and streamline curvature [129].

Another RANS model is the *transition SST* (*γ-Reθ*) model, which was extended based on the *k-ω SST* [130]. It has four-transport equations, which link *k-ω (SST)* equations with momentum thickness Reynolds number transition outset method (*Reθ*) and intermittency (*γ*) transport equations. The *transition SST* model is more precise than classical fully turbulent models due to its the ability to deal with the laminar-turbulent transition flow model where the separation of flow and stall phenomena occurred.

The Spalart-Allmaras (*SA*) is the simplest RANS turbulence model, which uses one transport equation. Where the computational of turbulence quantity is formulated by one transport equation, in which the kinematic eddy turbulent viscosity is the equation's variable [131]. This model was designed and optimized for a compressible flow over airfoils and wings for aerospace applications. It could simply imply a different type of grid for practical situations with including adverse pressure gradients where it gets easily stable and convergence of the solution[132]. On the way, the model could make significant diffusion, especially in regions of 3D vortices flow [133]. Different improvement work is done by Spalart and Shur [134], and Rahman et al. [135] to take into consideration the effects of rotation, near wall and reduction of the diffusion effect. The advantage of the fast convergence of this model reflected in the low computation time when compared to other turbulence models [132].

Large Eddy Simulation (LES) is another model developed to have a lower computationally demand than Direct Navier-Stokes. The first trial of LES in engineering has been done by Deardorff [136-139]. Unlike RANS models, the LES turbulence model has wider

applicability and more accurate results compared to the RANS model. Another advantage is decreasing the length of scales in LES approaches in which the turbulent is divided into two parts in the computational domain. The first part is the important large scales which was fully resolved, while the second part is the small sub-grid scales, which behave in a universal way, are modeled. The superiority of LES models uses in high Reynolds number turbulence models investigations and adequate prediction of complex flow than other turbulence models [140]. Unfortunately, the required computational time for the LES model is higher than the RANS model.

The Detached-Eddy Simulation (DES) was developed in 1997 [141] and applied for high Reynolds number with a massively separated flow [142]. The latter method is a blending model between LES and RANS approaches. Hence, LES is applied with external flow regions with massive separations, whereas the boundary layer is solved by RANS [143]. Travin et al. [144] described the DES as a single turbulence model that used unsteady three-dimensional numerical methods. Johansen et al. [145] found that using DES approaches does not improve the characteristic of the wind turbine did not been improved when using the DES method due to the long computational time.

4.2. Application of turbulence models used for aerodynamic simulation of the wind turbine

The numerical simulation of flow around the wind turbine is sensitive to the numerical models used for wind turbine design under operating conditions. The literature is abundant with various turbulence models that were used for validation of different numerical methods against experimental works. For example, Li et al. [146] used CFD Ship-lowa with a sliding mesh for NREL PHASE VI investigation of unsteady RANS model and DES model. The study found that the results of thrust forces and moments were different from the experimental work. However, using DES caused considerable improvements in the unsteady flow of the wind turbine.

Lanzafame et al.[147], Potsdam and Mavriplis [148], and Rajvanshi et al.[149] studied the numerical simulation of NREL PHASE VI using *k-ω SST* and *transition SST*. The results demonstrated the better capabilities of *transition SST* compared to *k-ω SST* with experimental work. In another work, Moshfeghi et al. [150] studied the effects of near-wall grid treatment on the aerodynamic performance of the wind turbine. NERL Phase VI model with eight cases was examined for a near-wall grid that used *k-ω SST* and *transition SST* turbulence models. Different wind speeds are used for predicting thrust forces and pressure coefficients. The thrust force results of *k-ω SST* were not in good agreement with the thrust values in test results. In general, the *k-ω SST* model is over predicting the performance of the wind turbine. However, *transition SST* behavior is different from the *k-ω SST* model, particularly in the inboard regions, but the outcomes are close to the experimental work.

k-ε turbulence models are used in studying the flow around the wind turbine and wake dynamic behavior. Kasmi and Masson [151]and Abelsalam et al. [152] performed a full-scale study of three wind turbines based on different *k-ε* turbulence models and

compared results with experimental work. The results showed that the modified k-ε is in better agreement with previous experimental measurements than standard k-ε. Different studies on the reliability of predicting wind turbine performance using different turbulence models. Rutten et al. [153] computed the NREL phase VI using two RANS models: k-ω, k-ω *SST*. The result showed that the k-ω *SST* turbulence model gives a better estimation for turbulent kinetic energy value when compared to k-ω. Abdulqadir et al. [154] investigated the reliability based on RANS and 12 turbulence models for predicting of NERL Phase VI wind turbine. All RANS numerical key performance coefficient at low tip speed ratios showed a good value when validated against experimental results. However, during high tip speed ratios, the poorest simulation results achieved by k-ω *SST*, whereas realizable k-ε showed relatively good results. You et al. [155] investigated the effect of different RANS turbulence models (Spalart-Allmaras, k-ω *SST*, and *transition SST*) on the estimation of the aerodynamic characteristic around the NREL phase VI blade rotor. The results demonstrated the ability of *transition SST* of capturing the laminar separation bubbles around the airfoil surface and rotor blade. Thus, the results of the k-ω Transition model has good agreement with experimental data due to a good prediction of the transition area of boundary layer. The numerical performance predicting of New Mexico wind turbine investigated the effect among RANS turbulence models using two different near-wall methods of high and low Reynolds number [156]. The RANS models used in the high Reynolds model are Spalart-Allmaras and k-ε *RNG*, while the models have been used for a low Reynold number are k-ω *SST* and k-ω Transition. All four models, under low wind speeds range, had a good prediction of the aerodynamic performance of the wind turbine. While increasing the wind speeds, more differences between models appear, the high Reynold model had better results compared with the low Reynolds model. A swirl effect was considered with wall function corrections, where the *RNG* k-ε turbulence model is recommended with increasing wind speed [156]. The following table shows the previous works of the CFD summary for HAWT.

Authors	Year	Turbine Type	Method/Tool	Transient /steady	Reynolds number	Numerical Turbulence model	Mesh (full or periodic)	Key investigated parameters	Comments
Sørensen et al. [157]	2002	NREL PHASE VI 2 bladed turbine	EllipSys3D CFD code	Transient	At the root and tip, the Reynolds number varies between $(0.7\text{-}1.4)10^6$ and $(1.0\text{-}1.1)10^6$, respectively.	*k-ω SST*	Using 90° Section with the periodic plane. 3.1,4.2 million cells for free and tunnel configuration	Validate computed value of flap and edge moments, aerodynamic coefficient, and pressure distribution during wind speed variation against the experimental results.	Airfoil type is S809. Diammeter10.068(m) In the study of aerodynamics, the influence of Tower and nacelle will be ignored. 0° yaw angle and 3° pitch angle.
Johansen et al. [145]	2002	NREL PHASE VI, 2 bladed turbine	EllipSys3D CFD code	Transient	Free Flow velocity V=20 m/s	DES, *k-ω SST*	Using 90° Section with the periodic plane. 8.9 million cells	Validate predicting values of the normal and tangential force coefficient distribution that focuses on static and dynamic stall regions with experimental NREL data.	Airfoil type is S809. Diammeter10.068(m) In the study of aerodynamics, the influence of Tower and nacelle will be ignored.
Duque et al.[158]	2003	NREL PHASE VI, 2 bladed turbine	OVERFLOW-D2 CAMRAD II code	Transient	Velocity=13,15, 20,25 m/s			OVERFLOW-2D predicted good results against experimental work in non-stall conditions	Yaw angle at 13°,30°,60°
Johansen and Sørensen [159]	2004	NREL PHASE VI, Danish 95 kW Tellus and Danish 500 kW. 3-bladed wind turbine.	BLADE ELEMENT MOMENTUM METHOD (BEM) & EllipSys3D CFD code	Transient	$Re=1*10^6$	DES, *k-ω SST*		Computed mechanical power using CFD has a good convenient with BEM.	Stall-regulated wind turbine 0° yaw angle. Derived new correction models from extracted aerofoil characteristic
Mandas et al. [160]	2006	Nordtank 41/500 turbine,500 kW 3-bladed turbine	Fluent	Steady	Free Flow velocity range 6.8-12 m/s	Spalart-Allmaras, *k-ω SST*	1.5 million Cells. 120° periodicity used for the rotor	Study how wind velocity variation effect shaft mechanical Torque and Tip speed ratio corresponding to Functions of power coefficient.	Fixed pitch, stall regulated. NACA 63-4xx Tower and nacelle will be ignored. Rotor diameter of 41 m. Good agreement of aerodynamic performance from CFD when compared with BEM.

Sezer-Uzol, and Long [161]	2006	NREL PHASE VI, 2 bladed turbine	PUMA2 solver	Transient	Velocity at 7,15 m/s	Large Eddy Simulations, (LES)	3.6 million rotating tetrahedral cells	The flow attached at case1,2 but in case 3 there is a massive separation with the entire blade	Different yaw cases: Case 1: 7m/s yaw angle 0°. Case 2: 7 m/s yaw angle 30°. Case 3:15 m/s yaw angle 0°.
Hu et al.[162]	2006	Three-bladed downwind rotor	Fluent	Steady	Mean velocity varies from 0-15 m/s	*RNG k-ε*	352,080 cells. 120° periodicity used for the rotor	Using Using the boundary layer analysis method to have a deep understanding of the essential physics of stall delay phenomena	NREL S809 airfoil. Diameter of 1(m) In 3D stall delay, Coriolis and centrifugal forces are important. Validated against Simms et al. [163]
Wußow et al.[164]	2007	3 bladed HAWT Type ENERCON E66	Fluent	Transient	Velocity range 8-12 m/s	LES	4.05 million cells Full blade simulated	Compared the local value of velocity magnitude and Turbulence intensity inside the wake with field measurement.	Validated against data which collected during "Deutsche Institut für Bautechnik" field project Tower include during simulation analysis.
Thumthae and Chitsomboon [165]	2009	NREL PHASE II 3-bladed wind turbine.	Fluent	Steady	Wind speeds at 7.2,8.0,9.0,10.5 m/s	*Standard k-ε*	120° periodicity used for the rotor	Find the optimal angle of attack which gets the greatest power output.	NREL S809 airfoil. The rotor diameter of 10.068 m 20 kW of constant 72 rpm Pitch angles are 4.12^{0},5.28^{0},6.66^{0},8.76^{0} Validated against NREL PHASE II.
Fletcher et al.[166]	2009	NREL PHASE VI, 2 bladed turbine		Steady	Wind speeds at 7,10,25 m/s	RANS equations. Vorticity Transport Model.		Study normal, tangential force and power coefficient.	Good ability of the Vorticity Transport Model for wake structure. Validated against NREL PHASE VI
Sørensen [167]	2009	NREL PHASE VI, 2 bladed turbine	EllipSys3D	Transient	Reynolds number of 7.2×10^{6}	*k-ω SST*, *transition SST*	512×128 cells	Used the *transition SST* for predicting lift and drag of two turbine	S809, NACA63-415 Variable turbulence intensity will vary from 1.20% to 0.38%. 0 yaw angle. Validated against NREL PHASE VI
Gómez-Iradi et al [168]	2009	NREL PHASE VI 2 bladed turbine		Transient	Velocity at 7,10,20 m/s	URANS	Different mesh distribution used for each case	Investigated the effect of the wind tunnel wall and blade/Tower interaction on aerodynamic of wind turbine	Validated against NREL PHASE VI. Compressible flow. Tower and nacelle included in the study.

Tachos et al[169]	2010	NREL PHASE VI 3 bladed turbine	Fluent	Steady	Velocity at 7.2 m/s	Spalart-Allmaras , *RNG k-ε , standard k-ε, k-ω SST*	4.2 million cells, 120°periodicity used for the rotor	Comparison for pressure distribution between different Turbulence models against experiment work.	Airfoil type is S809. Diammeter10.068(m) Incompressible Tower and nacelle will be ignored.
Fu and Farzaneh [170]	2010	NREL PHASE VI 3 bladed turbine	Fluent	Steady	Velocity at 7,10,13 m/s	*k-ε*	1.7 million cells, 120° periodicity used for the rotor	Model HAWT under the process of rime –ice accretion.	Airfoil type is S809. The rotor diammeter10.068(m) Different rotation speeds 5, 7.5 and 10 rad/s.
Bechmann et al.[171]	2011	MEXICO 3-bladed turbine	EllipSys3D	Steady	Velocity at 10,15,24 m/s	*k-ω SST*	120° periodicity used for the rotor	Validating aerodynamic forces against experiment.	4.5 m diameter DU91-W2-250, RISOE A21, NACA 64418
Lawson et al. [58]	2011	550 kW Two bladed turbine	STAR CCM+	Transient	Velocity at 0.5 m/s to 3.0 m/s.	*k-ω SST*	Used different mesh density , 90°periodicity used for the rotor	Study Pressure distribution, blade root flap of the wind turbine	NACA 63(1)-424
Elfarra et al. [172]	2014	NREL PHASE VI Two bladed turbine	Fine/Turbo of NUMECA	Transient	12 different wind speeds between 5 and 25 m/s	RANS *k-ε*	350,000 cells Using 90° Section with periodic plane	Comparison between optimized blade(with winglet) and the original blade(without winglet)	The optimize blade (with winglet) increased the power production by 9% compared to the original blade. Validated against NREL PHASE VI
Abdelsalam et al.[173]	2014	2 MW wind turbine	Fluent	Steady	Velocity at 8,10,12,14 m/s	*Standard k-ε*	Unstructured mesh CFD ICEM	Validated against El Kamsi[151]	The results showed that k-ε could give a good result if the blade modelled accurately.
Song and Perot [174]	2015	NREL PHASE VI Two bladed turbine	OpenFOAM-1.6-ext	Transient	Different wind speed =5 ,10 ,21 m/s,	RANS	10 million cells	Studied the 3D flow under separation conditions.	0 °yaw angle 3° tip pitch angle The rotation speed of 72 rpm.
Derakhshan and Tavaziani [175]	2015	NREL phase VI	Fluent	Steady	Low wind speed (5-20) m/s	Spalart-Allmaras *k-ω SST* k-ε	2,697,136 mesh	Validated against NREL phase VI	*k-ω SST* showed better results when compared to experimental values.
Sørensen et al. [176]	2016	MEXICO Three bladed turbine	EllipSys3D	steady	Velocity at 10,15,24 m/	*k-ω SST*	span-wise direction (129 cells) chord-wise direction (256 cells) normal direction (128 cells)	The results showed good agreement with experimental values.	The numerical results investigated the pressure distributions and wake characteristics.

Wang et al [177]	2016	WindPACT 1.5 MW	Fluent	steady	Velocity at (8,12,16,20,24) m/s	*k-ω SST*	5,460,679 cells	The model is validated against literature data test	
Menegozzo et al.[178]	2018	NREL phase VI Two bladed wind turbine	Fluent	Transient	Different wind velocity range	*k-ω SST*	8.5 million cells unstructured moving mesh strategy.	Validated against NREL phase VI	A numerical study of the extreme load has been investigated.

482

5. Conclusion remarks and challenging.

There are different challenges when using the wind turbine technology such as high competition between industries part [179], wind measurement devices accuracy[180], maintenance and operations problems [181-186], in addition to power and grid distribution challenges [187-189]. There are different solutions to improve the control system [190, 191], wind forecasting devices [192-194].

In general, the aerodynamics of the wind turbine was studied for more than two centuries. The aerodynamics of the wind turbine was studied for more than two centuries and previous studies ficysed mostly the challenges and solutions using experimental methods. However, the 3D simulation work is still in the earlier stage with many simplifications due to cost and complexity. This paper reviews the key points in the aerodynamic wind turbine design. The major conclusions of this review are:

- Accurate wind distribution data is essential in the design of wind turbine depending on specific site. Weibull and Rayleigh are two probability distribution functions that are commonly used to determine the occurrence frequency of wind speed. Until now, there are many works in this direction by development different models to compare the accuracy between these probability density function.
- Different parameters affected the design of wind turbines such as the HAWT power curve, tip speed ratio, Blade Plane shape. There are several research works to enhance the aerodynamic performance by decreasing cut-in speed, appropriate selection of tip speed ratio with taking into consideration the mechanical stress and noise.
- There are different families used in a modern wind turbine, selection of these airfoils depending on different considerations such as a lift to drag coefficient. Different research on design criteria of mixing airfoil to increase the efficiency of the wind turbine is a one of research topic.
- The simulation of HAWT using CFD is a very good tool in predicting aerodynamic performance, which accuracy depending on the selection of suitable turbulence models. Most of the current numerical work focuses on increasing the accuracy of CFD models of predicting aerodynamic performance by trying to solving constraints of cost and time consuming through simulation.

References

[1] J. Conti, P. Holtberg, J. Diefenderfer, A. LaRose, J.T. Turnure, L. Westfall. International energy outlook 2016 with projections to 2040. USDOE Energy Information Administration (EIA), Washington, DC (United States …2016.

[2] R.E. Sims, H.-H. Rogner, K. Gregory. Carbon emission and mitigation cost comparisons between fossil fuel, nuclear and renewable energy resources for electricity generation. Energy policy. 31 (2003) 1315-26.

[3] W.W.E.A. ". Wind Power Capacity Worldwide Reaches 597 GW, 50,1 GW added in 2018. February 25, 2019.

[4] H. Kaviani, A. Nejat. Aerodynamic noise prediction of a MW-class HAWT using shear wind profile. Journal of Wind Engineering and Industrial Aerodynamics. 168 (2017) 164-76.

[5] Z.N. Ashrafi, M. Ghaderi, A. Sedaghat. Parametric study on off-design aerodynamic performance of a horizontal axis wind turbine blade and proposed pitch control. Energy conversion and management. 93 (2015) 349-56.

[6] M. Lydia, S.S. Kumar, A.I. Selvakumar, G.E. Prem Kumar. A comprehensive review on wind turbine power curve modeling techniques. Renewable and Sustainable Energy Reviews. 30 (2014) 452-60.

[7] P. Tchakoua, R. Wamkeue, M. Ouhrouche, F. Slaoui-Hasnaoui, T.A. Tameghe, G. Ekemb. Wind turbine condition monitoring: State-of-the-art review, new trends, and future challenges. Energies. 7 (2014) 2595-630.

[8] B. Sanderse, S.P. van der Pijl, B. Koren. Review of computational fluid dynamics for wind turbine wake aerodynamics. Wind Energy. 14 (2011) 799-819.
[9] D. Infield, L. Freris. Renewable energy in power systems. John Wiley & Sons2020.
[10] C.-J. Bai, P.-W. Chen, W.-C. Wang. Aerodynamic design and analysis of a 10 kW horizontal-axis wind turbine for Tainan, Taiwan. Clean Technologies and Environmental Policy. 18 (2016) 1151-66.
[11] J.F. Manwell, J.G. McGowan, A.L. Rogers. Wind energy explained: theory, design and application. John Wiley & Sons2010.
[12] Y.A. Katsigiannis, G.S. Stavrakakis. Estimation of wind energy production in various sites in Australia for different wind turbine classes: A comparative technical and economic assessment. Renewable energy. 67 (2014) 230-6.
[13] G.M. Masters. Renewable and efficient electric power systems. John Wiley & Sons2013.
[14] P.A.C. Rocha, R.C. de Sousa, C.F. de Andrade, M.E.V. da Silva. Comparison of seven numerical methods for determining Weibull parameters for wind energy generation in the northeast region of Brazil. Applied Energy. 89 (2012) 395-400.
[15] J. Seguro, T. Lambert. Modern estimation of the parameters of the Weibull wind speed distribution for wind energy analysis. Journal of wind engineering and industrial aerodynamics. 85 (2000) 75-84.
[16] O.N. Laban, C.M. Maghanga, K. Joash. Determination of the Surface Roughness Parameter and Wind Shear Exponent of Kisii Region from the On-Site Measurement of Wind Profiles. Journal of Energy. 2019 (2019).
[17] L. Wang, M.E. Cholette, A.C. Tan, Y. Gu. A computationally-efficient layout optimization method for real wind farms considering altitude variations. Energy. 132 (2017) 147-59.
[18] M. Islam, R. Saidur, N. Rahim. Assessment of wind energy potentiality at Kudat and Labuan, Malaysia using Weibull distribution function. Energy. 36 (2011) 985-92.
[19] A. Krenn, H. Winkelmeier, R. Cattin, S. Müller, H. Truhetz, M. Biberacher, et al. Austrian wind atlas and wind potential analysis. DEWEK, available at: www windatlas at/downloads/20101117_Paper_Dewek pdf. (2010).
[20] A.N. Celik. A statistical analysis of wind power density based on the Weibull and Rayleigh models at the southern region of Turkey. Renewable energy. 29 (2004) 593-604.
[21] D. Mentis, S. Hermann, M. Howells, M. Welsch, S.H. Siyal. Assessing the technical wind energy potential in Africa a GIS-based approach. Renewable Energy. 83 (2015) 110-25.
[22] P.-C. Ma, Y. Zhang. Perspectives of carbon nanotubes/polymer nanocomposites for wind blade materials. Renewable and Sustainable Energy Reviews. 30 (2014) 651-60.
[23] H. Perez-Blanco. Optimization of Wind energy capture Using BET. ASME 2011 Turbo Expo: Turbine Technical Conference and Exposition. American Society of Mechanical Engineers Digital Collection2011. pp. 879-87.
[24] M.M. Duquette, K.D. Visser. Numerical implications of solidity and blade number on rotor performance of horizontal-axis wind turbines. J Sol Energy Eng. 125 (2003) 425-32.
[25] R. McKenna, P.O. vd Leye, W. Fichtner. Key challenges and prospects for large wind turbines. Renewable and Sustainable Energy Reviews. 53 (2016) 1212-21.
[26] T.M. Letcher. Wind energy engineering: a handbook for onshore and offshore wind turbines. Academic Press2017.
[27] S. Heier. Grid integration of wind energy: onshore and offshore conversion systems. John Wiley & Sons2014.
[28] I. Boldea, L.N. Tutelea. Electric machines: steady state, transients, and design with MATLAB. CRC press2009.
[29] M. Orabi, F. El-Sousy, H. Godah, M. Youssef. High-performance induction generator-wind turbine connected to utility grid. INTELEC 2004 26th Annual International Telecommunications Energy Conference. IEEE2004. pp. 697-704.
[30] L. Mishnaevsky Jr, O. Favorsky. Composite materials in wind energy technology. Thermal to Mechanical Energy Conversion: Engines and Requirements, EOLSS Publishers: Oxford, UK. (2011).
[31] T. Ashwill. Materials and innovations for large blade structures: research opportunities in wind energy technology. 50th AIAA/ASME/ASCE/AHS/ASC Structures, Structural Dynamics, and Materials Conference 17th AIAA/ASME/AHS Adaptive Structures Conference 11th AIAA No2009. p. 2407.
[32] R.W. Thresher, D.M. Dodge. Trends in the evolution of wind turbine generator configurations and systems. Wind Energy: An International Journal for Progress and Applications in Wind Power Conversion Technology. 1 (1998) 70-86.
[33] G. Sieros, P. Chaviaropoulos, J.D. Sørensen, B.H. Bulder, P. Jamieson. Upscaling wind turbines: theoretical and practical aspects and their impact on the cost of energy. Wind energy. 15 (2012) 3-17.
[34] A. Al-Abadi, Ö. Ertunç, F. Beyer, A. Delgado. Torque-matched aerodynamic shape optimization of HAWT rotor. Journal of Physics: Conference Series. IOP Publishing2014. p. 012003.
[35] A. Al-Abadi, Ö. Ertunç, H. Weber, A. Delgado. A design and optimization method for matching the torque of the wind turbines. Journal of Renewable and Sustainable Energy. 7 (2015) 023129.

[36] J.-J. Chattot. Optimization of wind turbines using helicoidal vortex model. J Sol Energy Eng. 125 (2003) 418-24.
[37] M. Jureczko, M. Pawlak, A. Mężyk. Optimisation of wind turbine blades. Journal of materials processing technology. 167 (2005) 463-71.
[38] J. Henriques, F.M. Da Silva, A. Estanqueiro, L. Gato. Design of a new urban wind turbine airfoil using a pressure-load inverse method. Renewable Energy. 34 (2009) 2728-34.
[39] A. Vardar, I. Alibas. Research on wind turbine rotor models using NACA profiles. Renewable Energy. 33 (2008) 1721-32.
[40] K. Ameku, B.M. Nagai, J.N. Roy. Design of a 3 kW wind turbine generator with thin airfoil blades. Experimental thermal and fluid science. 32 (2008) 1723-30.
[41] D. Leung, Y. Deng, M. Leung. Design optimization of a cost-effective micro wind turbine. WCE 2010-World Congress on Engineering 2010. International Association of Engineers.2010.
[42] H. Hirahara, M.Z. Hossain, M. Kawahashi, Y. Nonomura. Testing basic performance of a very small wind turbine designed for multi-purposes. Renewable energy. 30 (2005) 1279-97.
[43] X. Liu, L. Wang, X. Tang. Optimized linearization of chord and twist angle profiles for fixed-pitch fixed-speed wind turbine blades. Renewable Energy. 57 (2013) 111-9.
[44] C. Kong, J. Bang, Y. Sugiyama. Structural investigation of composite wind turbine blade considering various load cases and fatigue life. Energy. 30 (2005) 2101-14.
[45] S. Seo, S.-D. Oh, H.-Y. Kwak. Wind turbine power curve modeling using maximum likelihood estimation method. Renewable energy. 136 (2019) 1164-9.
[46] R.A. Kishore, S. Priya. Design and experimental verification of a high efficiency small wind energy portable turbine (SWEPT). Journal of wind engineering and industrial aerodynamics. 118 (2013) 12-9.
[47] R.K. Singh, M.R. Ahmed, M.A. Zullah, Y.-H. Lee. Design of a low Reynolds number airfoil for small horizontal axis wind turbines. Renewable energy. 42 (2012) 66-76.
[48] S. Derakhshan, A. Tavaziani, N. Kasaeian. Numerical shape optimization of a wind turbine blades using artificial bee colony algorithm. Journal of Energy Resources Technology. 137 (2015) 051210.
[49] R. Gasch, J. Twele. Wind power plants: fundamentals, design, construction and operation. Springer Science & Business Media2011.
[50] A. Scholbrock, P. Fleming, L. Fingersh, A. Wright, D. Schlipf, F. Haizmann, et al. Field testing LIDAR-based feed-forward controls on the NREL controls advanced research turbine. 51st AIAA Aerospace Sciences Meeting Including the New Horizons Forum and Aerospace Exposition2013. p. 818.
[51] S. Oerlemans, P. Sijtsma, B. Méndez López. Location and quantification of noise sources on a wind turbine. Journal of Sound and Vibration. 299 (2007) 869-83.
[52] W. Tong. Wind power generation and wind turbine design. WIT press2010.
[53] A. Sedaghat, M. Mirhosseini. Aerodynamic design of a 300 kW horizontal axis wind turbine for province of Semnan. Energy conversion and management. 63 (2012) 87-94.
[54] E. Hau, H. von Renouard. Wind turbines: fundamentals, technologies, application, economics. Springer2003.
[55] P. Devinant, T. Laverne, J. Hureau. Experimental study of wind-turbine airfoil aerodynamics in high turbulence. Journal of Wind Engineering and Industrial Aerodynamics. 90 (2002) 689-707.
[56] F. Bertagnolio, N.N. Sørensen, J. Johansen, P. Fuglsang. Wind turbine airfoil catalogue. (2001).
[57] H. Fupeng, L. Yuhong, C. Zuoyi. Suggestions for improving wind turbines blade characteristics. Wind Engineering. 25 (2001) 105-13.
[58] M.J. Lawson, Y. Li, D.C. Sale. Development and verification of a computational fluid dynamics model of a horizontal-axis tidal current turbine. ASME 2011 30th International Conference on Ocean, Offshore and Arctic Engineering. American Society of Mechanical Engineers Digital Collection2011. pp. 711-20.
[59] M. Yılmaz, H. Köten, E. Çetinkaya, Z. Coşar. A comparative CFD analysis of NACA0012 and NACA4412 airfoils. Journal of Energy Systems. 2 (2018) 145-59.
[60] P. Fuglsang, K.S. Dahl. Design of the new RISO-A1 airfoil family for wind turbines. EWEC-CONFERENCE-1999. pp. 134-7.
[61] P. Fuglsang, C. Bak. Development of the Risø wind turbine airfoils. Wind Energy: An International Journal for Progress and Applications in Wind Power Conversion Technology. 7 (2004) 145-62.
[62] K.S. Dahl, P. Fuglsang. Design of the wind turbine airfoil family RISØ-A-XX1998.
[63] W. Timmer, R. Rooij. Summary of the Delft University wind turbine dedicated airfoils. 41st aerospace sciences meeting and exhibit2003. p. 352.
[64] J.L. Tangler, D.M. Somers. NREL airfoil families for HAWTs. National Renewable Energy Lab., Golden, CO (United States)1995.
[65] D.M. Somers. S833, S834, and S835 Airfoils: November 2001--November 2002. National Renewable Energy Lab.(NREL), Golden, CO (United States)2005.

[66] E. Sagol, M. Reggio, A. Ilinca. Issues concerning roughness on wind turbine blades. Renewable and Sustainable Energy Reviews. 23 (2013) 514-25.
[67] D.M. Somers, J.L. Tangler. Wind-tunnel test of the S814 thick root airfoil. National Renewable Energy Lab., Golden, CO (United States)1995.
[68] R. Van Rooij, W. Timmer. Roughness sensitivity considerations for thick rotor blade airfoils. J Sol Energy Eng. 125 (2003) 468-78.
[69] R. Lanzafame, M. Messina. Design and performance of a double-pitch wind turbine with non-twisted blades. Renewable Energy. 34 (2009) 1413-20.
[70] J. Laursen, P. Enevoldsen, S. Hjort. 3D CFD rotor computations of a multi-megawatt HAWT rotor. Proceedings of the European Wind Energy Conference, Milan, Italy2007.
[71] J.-H. Jeong, S.-H. Kim. CFD investigation on the flatback airfoil effect of 10 MW wind turbine blade. Journal of Mechanical Science and Technology. 32 (2018) 2089-97.
[72] M.R. Ahmed, S. Narayan, M.A. ZULLAH, Y.-H. Lee. Experimental and numerical studies on a low Reynolds number airfoil for wind turbine blades. Journal of Fluid Science and Technology. 6 (2011) 357-71.
[73] M.A. Sayed, H.A. Kandil, A. Shaltot. Aerodynamic analysis of different wind-turbine-blade profiles using finite-volume method. Energy conversion and Management. 64 (2012) 541-50.
[74] C. Sicot, P. Devinant, T. Laverne, S. Loyer, J. Hureau. Experimental study of the effect of turbulence on horizontal axis wind turbine aerodynamics. Wind energy. 9 (2006) 361-70.
[75] J. Delnero, J. Marañon di Leo, F. Bacchi, J. Colman, U. Boldes. Experimental determination of the influence of turbulent scale on the lift and drag coefficients of low Reynolds number airfoils. Latin American applied research. 35 (2005) 183-8.
[76] K.E. Swalwell, J. Sheridan, W. Melbourne. The effect of turbulence intensity on stall of the NACA 0021 aerofoil. 14th Australasian fluid mechanics conference2001. pp. 10-4.
[77] J.W. Larsen, S.R. Nielsen, S. Krenk. Dynamic stall model for wind turbine airfoils. Journal of Fluids and Structures. 23 (2007) 959-82.
[78] J.A. Hoffmann. Effects of freestream turbulence on the performance characteristics of an airfoil. AIAA journal. 29 (1991) 1353-4.
[79] Y. Kamada, T. Maeda, J. Murata, T. Toki, A. Tobuchi. Effects of turbulence intensity on dynamic characteristics of wind turbine airfoil. Journal of Fluid Science and Technology. 6 (2011) 333-41.
[80] G. Eke, J. Onyewudiala. Optimization of wind turbine blades using genetic algorithm. Global Journal of Research In Engineering. 10 (2010).
[81] D. Berg, J. Zayas. Aerodynamic and aeroacoustic properties of flatback airfoils. 46th AIAA Aerospace Sciences Meeting and Exhibit2008. p. 1455.
[82] M. McWilliam, C. Crawford. Manufacturing Defect Effects on Bend-Twist Coupled Wind Turbine Blades. 51st AIAA Aerospace Sciences Meeting including the New Horizons Forum and Aerospace Exposition2013. p. 1062.
[83] S.G. Lee, S.J. Park, K.S. Lee, C. Chung. Performance prediction of NREL (National Renewable Energy Laboratory) Phase VI blade adopting blunt trailing edge airfoil. Energy. 47 (2012) 47-61.
[84] S.-H. Kim, H.-J. Bang, H.-K. Shin, M.-S. Jang. Composite structural analysis of flat-back shaped blade for multi-MW class wind turbine. Applied Composite Materials. 21 (2014) 525-39.
[85] G.R. Fischer, T. Kipouros, A.M. Savill. Multi-objective optimisation of horizontal axis wind turbine structure and energy production using aerofoil and blade properties as design variables. Renewable Energy. 62 (2014) 506-15.
[86] L.I. Lago, F.L. Ponta, A.D. Otero. Analysis of alternative adaptive geometrical configurations for the NREL-5 MW wind turbine blade. Renewable Energy. 59 (2013) 13-22.
[87] D.L. Kahn, C. van Dam, D.E. Berg. Trailing edge modifications for flatback airfoils. Sandia National Laboratories2008.
[88] J.P. Baker, C. Van Dam. Drag reduction of a blunt trailing-edge airfoil. University of California, Davis2009.
[89] A. Cooperman, A. McLennan, J. Baker, C. van Dam, R. Chow. Aerodynamic performance of thick blunt trailing edge airfoils. 28th AIAA Applied Aerodynamics Conference2010. p. 4228.
[90] R. Chow, C. Van Dam. Computational investigations of blunt trailing-edge and twist modifications to the inboard region of the NREL 5 MW rotor. Wind Energy. 16 (2013) 445-58.
[91] S. Schreck, L. Fingersh, K. Siegel, M. Singh, P. Medina. Rotational Augmentation on a 2.3 MW Rotor Blade with Thick Flatback Airfoil Cross Sections. 51st AIAA Aerospace Sciences Meeting including the New Horizons Forum and Aerospace Exposition2013. p. 915.
[92] J.P. Murcia, Á. Pinilla. CFD analysis of blunt trailing edge airfoils obtained with several modification methods. Revista de Ingeniería. (2011) 14-24.

[93] K. Standish, C. Van Dam. Aerodynamic analysis of blunt trailing edge airfoils. Journal of Solar Energy Engineering. 125 (2003) 479-87.
[94] S. Law, G. Gregorek. Wind tunnel evaluation of a truncated NACA 64-621 airfoil for wind turbine applications. (1987).
[95] K. Homsrivaranon. Investigation of Active Flow Control on an Extremely Thick Wind Turbine Airfoil. University of Kansas2016.
[96] T.-t. Zhang, W. Huang, Z.-g. Wang, L. Yan. A study of airfoil parameterization, modeling, and optimization based on the computational fluid dynamics method. Journal of Zhejiang University-SCIENCE A. 17 (2016) 632-45.
[97] J. Baker, E. Mayda, C. Van Dam. Experimental analysis of thick blunt trailing-edge wind turbine airfoils. Journal of solar energy engineering. 128 (2006) 422-31.
[98] T. Göçmen, B. Özerdem. Airfoil optimization for noise emission problem and aerodynamic performance criterion on small scale wind turbines. Energy. 46 (2012) 62-71.
[99] T. Kim, M. Jeon, S. Lee, H. Shin. Numerical simulation of flatback airfoil aerodynamic noise. Renewable energy. 65 (2014) 192-201.
[100] C.M. Velte, M.O.L. Hansen, K.E. Meyer, P. Fuglsang. Evaluation of the Performance of Vortex Generators on the DU 91-W2-250 Profile using Stereoscopic PIV. International Symposium on Energy, Informatics and Cybernetics: Focus Symposium in the 12th World Multiconference on Systemics, Cybernetics and Informatics (WMSCI 2008)2008.
[101] L.P. Chamorro, R. Arndt, F. Sotiropoulos. Drag reduction of large wind turbine blades through riblets: Evaluation of riblet geometry and application strategies. Renewable Energy. 50 (2013) 1095-105.
[102] O. Ceyhan, W. Timmer. Experimental evaluation of a non-conventional flat back thick airfoil concept for large offshore wind turbines. 2018 Applied Aerodynamics Conference2018. p. 3827.
[103] T. Kim, S. Lee. Aeroacoustic simulations of a blunt trailing-edge wind turbine airfoil. Journal of Mechanical Science and Technology. 28 (2014) 1241-9.
[104] P. Fuglsang, O. Sangill, P. Hansen. Design of a 21 m blade with risø-a1 airfoils for active stall controlled wind turbines2002.
[105] Z. Lubosny, J.W. Bialek. Supervisory control of a wind farm. IEEE Transactions on Power Systems. 22 (2007) 985-94.
[106] K. Gharali, D.A. Johnson. Numerical modeling of an S809 airfoil under dynamic stall, erosion and high reduced frequencies. Applied Energy. 93 (2012) 45-52.
[107] K. Johnson, J.-W. van Wingerden, M.J. Balas, D.-P. Molenaar. Special Issue on Past, present and future modeling and control of wind turbines. Mechatronics (Oxford). 21 (2011).
[108] M.-H. Chiang. A novel pitch control system for a wind turbine driven by a variable-speed pump-controlled hydraulic servo system. Mechatronics. 21 (2011) 753-61.
[109] A.P. Deshmukh, J.T. Allison. Multidisciplinary dynamic optimization of horizontal axis wind turbine design. Structural and Multidisciplinary Optimization. 53 (2016) 15-27.
[110] I. Munteanu, A.I. Bratcu, N.-A. Cutululis, E. Ceanga. Optimal control of wind energy systems: towards a global approach. Springer Science & Business Media2008.
[111] N. Wang, K.E. Johnson, A.D. Wright. Comparison of strategies for enhancing energy capture and reducing loads using LIDAR and feedforward control. IEEE Transactions on Control Systems Technology. 21 (2013) 1129-42.
[112] W. Xudong, W.Z. Shen, W.J. Zhu, J.N. Sørensen, C. Jin. Shape optimization of wind turbine blades. Wind Energy: An International Journal for Progress and Applications in Wind Power Conversion Technology. 12 (2009) 781-803.
[113] M. Soltani, R. Wisniewski, P. Brath, S. Boyd. Load reduction of wind turbines using receding horizon control. 2011 IEEE international conference on control applications (CCA). IEEE2011. pp. 852-7.
[114] J. Johansen, H.A. Madsen, M. Gaunaa, C. Bak, N.N. Sørensen. Design of a wind turbine rotor for maximum aerodynamic efficiency. Wind Energy: An International Journal for Progress and Applications in Wind Power Conversion Technology. 12 (2009) 261-73.
[115] R.N. Pinto, A. Afzal, L.V. D'Souza, Z. Ansari, A.M. Samee. Computational fluid dynamics in turbomachinery: a review of state of the art. Archives of Computational Methods in Engineering. 24 (2017) 467-79.
[116] R. Mikkelsen, J.N. Sørensen, S. Øye, N. Troldborg. Analysis of power enhancement for a row of wind turbines using the actuator line technique. Journal of Physics: Conference Series. IOP Publishing2007. p. 012044.
[117] H. Snel. Review of aerodynamics for wind turbines. Wind Energy: An International Journal for Progress and Applications in Wind Power Conversion Technology. 6 (2003) 203-11.
[118] P. Zhou. CFD Simulation of the Wind Turbine Wake Under Different Atmospheric Boundary Conditions. Purdue University2017.

[119] S. Schmidt, D. McIver, H.M. Blackburn, M. Rudman, G. Nathan. Spectral element based simulation of turbulent pipe flow. 14th A/Asian Fluid Mech Conf2001.
[120] A. Sargsyan. Simulation and modeling of flow field around a horizontal axis wind turbine (HAWT) using RANS method. Florida Atlantic University2010.
[121] B.E. Launder, B. Sharma. Application of the energy-dissipation model of turbulence to the calculation of flow near a spinning disc. Letters in heat and mass transfer. 1 (1974) 131-7.
[122] T.-H. Shih, W.W. Liou, A. Shabbir, Z. Yang, J. Zhu. A new k-epsilon eddy viscosity model for high Reynolds number turbulent flows: Model development and validation. (1994).
[123] V. Yakhot, S. Orszag, S. Thangam, T. Gatski, C. Speziale. Development of turbulence models for shear flows by a double expansion technique. Physics of Fluids A: Fluid Dynamics. 4 (1992) 1510-20.
[124] V. Yakhot, S.A. Orszag. Renormalization group analysis of turbulence. I. Basic theory. Journal of scientific computing. 1 (1986) 3-51.
[125] M. Mohamed. Performance investigation of H-rotor Darrieus turbine with new airfoil shapes. Energy. 47 (2012) 522-30.
[126] A. Mielke, J. Naumann. On the existence of global-in-time weak solutions and scaling laws for Kolmogorov's two-equation model of turbulence. arXiv preprint arXiv:180102039. (2018).
[127] D.C. Wilcox. Formulation of the kw turbulence model revisited. AIAA journal. 46 (2008) 2823-38.
[128] F.R. Menter. Review of the shear-stress transport turbulence model experience from an industrial perspective. International journal of computational fluid dynamics. 23 (2009) 305-16.
[129] P.E. Smirnov, F.R. Menter. Sensitization of the SST turbulence model to rotation and curvature by applying the Spalart–Shur correction term. Journal of turbomachinery. 131 (2009).
[130] R.B. Langtry, F.R. Menter. Correlation-based transition modeling for unstructured parallelized computational fluid dynamics codes. AIAA journal. 47 (2009) 2894-906.
[131] P. Spalart, S. Allmaras. A one-equation turbulence model for aerodynamic flows. 30th aerospace sciences meeting and exhibit1992. p. 439.
[132] A. Bouhelal, A. Smaïli, C. Masson, O. Guerri. Effects of Surface Roughness on Aerodynamic Performance of Horizontal Axis Wind Turbines. The 25th Annual Conference of the Computational Fluid Dynamics Society of Canada, CFD2017-337, University of Windsor2017. pp. 18-21.
[133] T.B. Gatski, C.L. Rumsey, R. Manceau. Current trends in modelling research for turbulent aerodynamic flows. Philosophical Transactions of the Royal Society A: Mathematical, Physical and Engineering Sciences. 365 (2007) 2389-418.
[134] P. Spalart, M. Shur. On the sensitization of turbulence models to rotation and curvature. Aerospace Science and Technology. 1 (1997) 297-302.
[135] M. Rahman, T. Siikonen, R. Agarwal. Improved low-Reynolds-number one-equation turbulence model. AIAA journal. 49 (2011) 735-47.
[136] J.W. Deardorff. A numerical study of three-dimensional turbulent channel flow at large Reynolds numbers. Journal of Fluid Mechanics. 41 (1970) 453-80.
[137] R.H. Kraichnan. Eddy viscosity in two and three dimensions. Journal of the atmospheric sciences. 33 (1976) 1521-36.
[138] J.R. Chasnov. Simulation of the Kolmogorov inertial subrange using an improved subgrid model. Physics of Fluids A: Fluid Dynamics. 3 (1991) 188-200.
[139] U. Piomelli. High Reynolds number calculations using the dynamic subgrid-scale stress model. Physics of Fluids A: Fluid Dynamics. 5 (1993) 1484-90.
[140] J. Fröhlich, C.P. Mellen, W. Rodi, L. Temmerman, M.A. Leschziner. Highly resolved large-eddy simulation of separated flow in a channel with streamwise periodic constrictions. Journal of Fluid Mechanics. 526 (2005) 19-66.
[141] P.R. Spalart. Comments on the feasibility of LES for wings, and on a hybrid RANS/LES approach. Proceedings of first AFOSR international conference on DNS/LES. Greyden Press1997.
[142] P.R. Spalart. Detached-eddy simulation. Annual review of fluid mechanics. 41 (2009) 181-202.
[143] O. Verhoeven. Trailing Edge Noise Simulations: Using IDDES in OpenFOAM. (2011).
[144] A. Travin, M. Shur, M. Strelets, P. Spalart. Detached-eddy simulations past a circular cylinder. Flow, turbulence and combustion. 63 (2000) 293-313.
[145] J. Johansen, N.N. Sørensen, J. Michelsen, S. Schreck. Detached-eddy simulation of flow around the NREL Phase VI blade. Wind Energy: An International Journal for Progress and Applications in Wind Power Conversion Technology. 5 (2002) 185-97.
[146] Y. Li, K.-J. Paik, T. Xing, P.M. Carrica. Dynamic overset CFD simulations of wind turbine aerodynamics. Renewable Energy. 37 (2012) 285-98.

[147] R. Lanzafame, S. Mauro, M. Messina. Wind turbine CFD modeling using a correlation-based transitional model. Renewable Energy. 52 (2013) 31-9.
[148] M. Potsdam, D. Mavriplis. Unstructured mesh CFD aerodynamic analysis of the NREL Phase VI rotor. 47th AIAA Aerospace Sciences Meeting including The New Horizons Forum and Aerospace Exposition2009. p. 1221.
[149] D. Rajvanshi, R. Baig, R. Pandya, K. Nikam. Wind turbine blade aerodynamics and performance analysis using numerical simulations. 11th Asian International Conference on Fluid Machinery2011.
[150] M. Moshfeghi, Y.J. Song, Y.H. Xie. Effects of near-wall grid spacing on SST-K-ω model using NREL Phase VI horizontal axis wind turbine. Journal of Wind Engineering and Industrial Aerodynamics. 107 (2012) 94-105.
[151] A. El Kasmi, C. Masson. An extended k–ε model for turbulent flow through horizontal-axis wind turbines. Journal of Wind Engineering and Industrial Aerodynamics. 96 (2008) 103-22.
[152] A.M. AbdelSalam, V. Ramalingam. Wake prediction of horizontal-axis wind turbine using full-rotor modeling. Journal of Wind Engineering and Industrial Aerodynamics. 124 (2014) 7-19.
[153] M. Rütten, J. Penneçot, C. Wagner. Unsteady Numerical Simulation of the Turbulent Flow around a Wind Turbine. Progress in Turbulence III. Springer2009. pp. 103-6.
[154] S.A. Abdulqadir, H. Iacovides, A. Nasser. The physical modelling and aerodynamics of turbulent flows around horizontal axis wind turbines. Energy. 119 (2017) 767-99.
[155] J.Y. You, D.O. Yu, O.J. Kwon. Effect of turbulence models on predicting HAWT rotor blade performances. Journal of Mechanical Science and Technology. 27 (2013) 3703-11.
[156] A. Bouhelal, A. Smaili, O. Guerri, C. Masson. Numerical investigation of turbulent flow around a recent horizontal axis wind Turbine using low and high Reynolds models. Journal of Applied Fluid Mechanics. 11 (2018) 151-64.
[157] N.N. Sørensen, J. Michelsen, S. Schreck. Navier–Stokes predictions of the NREL phase VI rotor in the NASA Ames 80 ft× 120 ft wind tunnel. Wind Energy: An International Journal for Progress and Applications in Wind Power Conversion Technology. 5 (2002) 151-69.
[158] E.P. Duque, M.D. Burklund, W. Johnson. Navier-Stokes and comprehensive analysis performance predictions of the NREL phase VI experiment. J Sol Energy Eng. 125 (2003) 457-67.
[159] J. Johansen, N.N. Sørensen. Aerofoil characteristics from 3D CFD rotor computations. Wind Energy: An International Journal for Progress and Applications in Wind Power Conversion Technology. 7 (2004) 283-94.
[160] N. Mandas, F. Cambuli, C.E. Carcangiu. Numerical prediction of horizontal axis wind turbine flow. University of Caglairi, EWEC. (2006).
[161] N. Sezer-Uzol, L. Long. 3-D time-accurate CFD simulations of wind turbine rotor flow fields. 44th AIAA Aerospace Sciences Meeting and Exhibit2006. p. 394.
[162] D. Hu, O. Hua, Z. Du. A study on stall-delay for horizontal axis wind turbine. Renewable Energy. 31 (2006) 821-36.
[163] D. Simms, M. Robinson, M. Hand, L. Fingersh. A comparison of baseline aerodynamic performance of optimally-twisted versus non-twisted HAWT blades. National Renewable Energy Lab., Golden, CO (United States)1995.
[164] S. Wußow, L. Sitzki, T. Hahm. 3D-simulation of the turbulent wake behind a wind turbine. Journal of Physics: Conference Series. IOP Publishing2007. p. 012033.
[165] C. Thumthae, T. Chitsomboon. Optimal angle of attack for untwisted blade wind turbine. Renewable energy. 34 (2009) 1279-84.
[166] T.M. Fletcher, R. Brown, D.H. Kim, O.J. Kwon. Predicting wind turbine blade loads using vorticity transport and RANS methodologies. European Wind Energy Conference and Exhibition, EWEC 20092009.
[167] N.N. Sørensen. CFD modelling of laminar-turbulent transition for airfoils and rotors using the γ− model. Wind Energy: An International Journal for Progress and Applications in Wind Power Conversion Technology. 12 (2009) 715-33.
[168] S. Gomez-Iradi, R. Steijl, G. Barakos. Development and validation of a CFD technique for the aerodynamic analysis of HAWT. Journal of Solar Energy Engineering. 131 (2009).
[169] N. Tachos, A. Filios, D. Margaris. A comparative numerical study of four turbulence models for the prediction of horizontal axis wind turbine flow. Proceedings of the Institution of Mechanical Engineers, Part C: Journal of Mechanical Engineering Science. 224 (2010) 1973-9.
[170] P. Fu, M. Farzaneh. A CFD approach for modeling the rime-ice accretion process on a horizontal-axis wind turbine. Journal of Wind Engineering and Industrial Aerodynamics. 98 (2010) 181-8.
[171] A. Bechmann, N.N. Sørensen, F. Zahle. CFD simulations of the MEXICO rotor. Wind Energy. 14 (2011) 677-89.
[172] M.A. Elfarra, N. Sezer-Uzol, I.S. Akmandor. NREL VI rotor blade: numerical investigation and winglet design and optimization using CFD. Wind Energy. 17 (2014) 605-26.

[173] A.M. Abdelsalam, K. Boopathi, S. Gomathinayagam, S.H.K. Kumar, V. Ramalingam. Experimental and numerical studies on the wake behavior of a horizontal axis wind turbine. Journal of Wind Engineering and Industrial Aerodynamics. 128 (2014) 54-65.
[174] Y. Song, J.B. Perot. Cfd simulation of the nrel phase vi rotor. Wind engineering. 39 (2015) 299-309.
[175] S. Derakhshan, A. Tavaziani. Study of wind turbine aerodynamic performance using numerical methods. Journal of Clean Energy Technologies. 3 (2015) 83-90.
[176] N.N. Sørensen, F. Zahle, K. Boorsma, G. Schepers. CFD computations of the second round of MEXICO rotor measurements. Journal of Physics: Conference Series. IOP Publishing2016. p. 022054.
[177] L. Wang, R. Quant, A. Kolios. Fluid structure interaction modelling of horizontal-axis wind turbine blades based on CFD and FEA. Journal of Wind Engineering and Industrial Aerodynamics. 158 (2016) 11-25.
[178] L. Menegozzo, A. Dal Monte, E. Benini, A. Benato. Small wind turbines: A numerical study for aerodynamic performance assessment under gust conditions. Renewable energy. 121 (2018) 123-32.
[179] M. Bolinger, R. Wiser. Wind power price trends in the United States: struggling to remain competitive in the face of strong growth. Energy Policy. 37 (2009) 1061-71.
[180] G. Giebel, R. Brownsword, G. Kariniotakis, M. Denhard, C. Draxl. The state-of-the-art in short-term prediction of wind power: A literature overview. (2011).
[181] M. Albadi, E. El-Saadany. Overview of wind power intermittency impacts on power systems. Electric power systems research. 80 (2010) 627-32.
[182] A. Cavallo. Controllable and affordable utility-scale electricity from intermittent wind resources and compressed air energy storage (CAES). Energy. 32 (2007) 120-7.
[183] B.K. Sovacool. The intermittency of wind, solar, and renewable electricity generators: Technical barrier or rhetorical excuse? Utilities Policy. 17 (2009) 288-96.
[184] F. Spinato, P.J. Tavner, G.J. Van Bussel, E. Koutoulakos. Reliability of wind turbine subassemblies. IET Renewable Power Generation. 3 (2009) 387-401.
[185] C.A. Walford. Wind turbine reliability: understanding and minimizing wind turbine operation and maintenance costs. Sandia National Laboratories2006.
[186] S. Faulstich, B. Hahn, P.J. Tavner. Wind turbine downtime and its importance for offshore deployment. Wind energy. 14 (2011) 327-37.
[187] G. Boyle. Renewable electricity and the grid: the challenge of variability. Routledge2009.
[188] R. Piwko, N. Miller, J. Sanchez-Gasca, X. Yuan, R. Dai, J. Lyons. Integrating large wind farms into weak power grids with long transmission lines. 2006 CES/IEEE 5th International Power Electronics and Motion Control Conference. IEEE2006. pp. 1-7.
[189] R. Perveen, N. Kishor, S.R. Mohanty. Off-shore wind farm development: Present status and challenges. Renewable and Sustainable Energy Reviews. 29 (2014) 780-92.
[190] T.K. Barlas, G.A. van Kuik. Review of state of the art in smart rotor control research for wind turbines. Progress in Aerospace Sciences. 46 (2010) 1-27.
[191] E. Bossanyi, B. Savini, M. Iribas, M. Hau, B. Fischer, D. Schlipf, et al. Advanced controller research for multi-MW wind turbines in the UPWIND project. Wind Energy. 15 (2012) 119-45.
[192] F.P.G. Márquez, A.M. Tobias, J.M.P. Pérez, M. Papaelias. Condition monitoring of wind turbines: Techniques and methods. Renewable Energy. 46 (2012) 169-78.
[193] Z. Hameed, Y. Hong, Y. Cho, S. Ahn, C. Song. Condition monitoring and fault detection of wind turbines and related algorithms: A review. Renewable and Sustainable energy reviews. 13 (2009) 1-39.
[194] F. Blaabjerg, K. Ma. Future on power electronics for wind turbine systems. IEEE Journal of emerging and selected topics in power electronics. 1 (2013) 139-52.
https://wwindea.org/blog/2019/02/25/wind-power-capacity-worldwide-reaches-600-gw-539-gw-added-in-2018/